Shielding effects of myelin sheath on axolemma depolarization under transverse electric field stimulation

Hui Ye [Corresp., 1] , **Jeffrey Ng** [1]

[1] Department of Biology, Loyola University of Chicago, Chicago, United States

Corresponding Author: Hui Ye
Email address: hye1@luc.edu

Axonal stimulation with electric currents is an effective method for controlling neural activity. An electric field parallel to the axon is widely accepted as the predominant component in the activation of an axon. However, recent studies indicate that the transverse component to the axolemma is also effective in depolarizing the axon. To quantitatively investigate the amount of axolemma polarization induced by a transverse electric field, we computed the transmembrane potential (Vm) for a conductive body that represents an unmyelinated axon (or the bare axon between the myelin sheath in a myelinated axon). We also computed the transmembrane potential of the sheath-covered axonal segment in a myelinated axon. We then systematically analyzed the biophysical factors that affect axonal polarization under transverse electric stimulation for both the bare and sheath-covered axons. Geometrical patterns of polarization of both axon types were dependent on field properties (magnitude and field orientation to the axon). Polarization of both axons was also dependent on their axolemma radii and electrical conductivities. The myelin provided a significant "shielding effect" against the transverse electric fields, preventing excessive axolemma depolarization. Demyelination could allow for prominent axolemma depolarization in the transverse electric field, via a significant increase in myelin conductivity. This shifts the voltage drop of the myelin sheath to the axolemma. Pathological changes at a cellular level should be considered when electric fields are used for the treatment of demyelination diseases. The calculated term for membrane polarization (Vm) could be used to modify the current cable equation that describes axon excitation by an external electric field to account for the activating effects of both parallel and transverse fields surrounding the target axon.

1   **Shielding effects of myelin sheath on axolemma depolarization under transverse electric field**

2   **stimulation**

3   Hui Ye, Jeffrey Ng

4   Department of Biology, Loyola University Chicago, 1032 W. Sheridan Rd., Chicago, IL 60660

5   Correspondence:

6   Hui Ye, Ph.D.

7   Department of Biology

8   Loyola University Chicago

9   Quinlan Life Sciences Education and Research Center

10   1032 W. Sheridan Rd., Chicago, IL 60660

11   Tel (773) 508-2720

12   Hui Ye: hye1@luc.edu

14   **ABSTRACT**

15   Axonal stimulation with electric currents is an effective method for controlling neural activity. An

16   electric field parallel to the axon is widely accepted as the predominant component in the activation

17   of an axon. However, recent studies indicate that the transverse component to the axolemma is

18   also effective in depolarizing the axon. To quantitatively investigate the amount of axolemma

19   polarization induced by a transverse electric field, we computed the transmembrane potential (Vm)

20   for a conductive body that represents an unmyelinated axon (or the bare axon between the myelin

21   sheath in a myelinated axon). We also computed the transmembrane potential of the sheath-

22   covered axonal segment in a myelinated axon. We then systematically analyzed the biophysical

23   factors that affect axonal polarization under transverse electric stimulation for both the bare and

24   sheath-covered axons. Geometrical patterns of polarization of both axon types were dependent on

25   field properties (magnitude and field orientation to the axon). Polarization of both axons was also

26   dependent on their axolemma radii and electrical conductivities. The myelin provided a significant

27   "shielding effect" against the transverse electric fields, preventing excessive axolemma

28   depolarization. Demyelination could allow for prominent axolemma depolarization in the

29   transverse electric field, via a significant increase in myelin conductivity. This shifts the voltage

30   drop of the myelin sheath to the axolemma. Pathological changes at a cellular level should be

31   considered when electric fields are used for the treatment of demyelination diseases. The

32   calculated term for membrane polarization (Vm) could be used to modify the current cable equation

33   that describes axon excitation by an external electric field to account for the activating effects of

34   both parallel and transverse fields surrounding the target axon.

INTRODUCTION

36   Electrical stimulation of nerve cells was first reported by Luigi Galvani in 1780 (Galvani

37   1791), who accidently found that muscles from a dead frog would twitch when touched with a

38   charged metal scalpel, a discovery that sparked the appreciation of electricity in relation to

39   animation — or life. Today, electric stimulation of neurons in the peripheral or central nervous

40   systems have been widely utilized for controlling neural network activity (Selimbeyoglu & Parvizi

41   2010), synaptic transmission (Nowak & Bullier 1998), and pain (Coderre et al. 1993). Electric

42   currents can also be generated via magneto-electric induction with magnetic coils for non-invasive

43   control of neural activity (Maccabee et al. 1991; Maccabee et al. 1993; Ye et al. 2011; Ye et al.

44   2010; Ye & Steiger 2015).

45   An electric field surrounding a straight nerve axon can be separated into two components:

46   one parallel to ($E_{//}$) and the other perpendicular (traversal, $E_{\perp}$) to the axon. The $E_{//}$ is widely

47   regarded as the predominant factor that activates the axons (Basser et al. 1992; Roth & Basser

48   1990), which is supported by numerous experimental results (Amassian et al. 1989; Basser & Roth

49   2000). Consequently, theoretical analyses of electrical activation have predominately been focused

50   on computing $E_{//}$ along a fiber (Esselle & Stuchly 1994; Esselle & Stuchly 1995; Nagarajan &

51   Durand 1995; Ravazzani et al. 1996; Roth & Basser 1990; Roth et al. 1990). The current cable

52   equation, $\lambda^2 \dfrac{\partial^2 \varphi_m}{\partial x^2} - \tau \dfrac{\partial \varphi_m}{\partial t} - \varphi_m = -\lambda^2 \dfrac{\partial V_e}{\partial x^2}$, which describes axonal activation, contains only the

53   axial term ($E_{//}$). Here, $\lambda^2 = \dfrac{R_m c}{2R_i}$ and $\tau = R_m C_m$ are the space and time constants, respectively. φ_m

54   is the transmembrane potential and V_e is the extracellular electric field applied to the fiber. It is

55   nonzero only if $E_{//}$ is nonzero. The surface resistance and capacitance of the membrane are R_m

56   and C_m, respectively. The intracellular resistivity is R_i and the fiber radius is c. This simplification

57   facilities the rapid calculation of neural activation. However, it ignores the presence of the cell,

58 which perturbs the local extracellular electric field. It also ignores the mutual interactions between

59 the neurons and the applied electric field (Ye & Steiger 2015), mainly the electric field that directly

60 penetrates and depolarizes the cell membrane, or $E_\perp$.

61 Transversal field for membrane polarization

62 Mounting evidence from experimental and simulation studies support the notion that cell

63 membranes can be polarized by transversal electric fields. An electric field that penetrates the cell

64 membrane was directly observed to cause polarization in hippocampal neurons (Bikson et al.

65 2001), in neural stem cells (Zhao et al. 2015), and in oocytes (Lee & Grill 2005). When $E_\perp$ is

66 extremely strong, it can even cause membrane instability and pore formation (Bingham et al.

67 2010). Analytical computations of the transverse membrane potential under electric stimulation

68 started as early as the 1950s (Fricke 1953; Schwan 1957) for a simple cellular shape. Recent works

69 have calculated membrane polarization by the transverse field in cells with more complex

70 geometry (Kotnik & Miklavcic 2000a; Kotnik & Miklavcic 2000b), and by the transverse electric

71 field induced by time-varying magnetic field (Ye et al. 2007; Ye et al. 2011).

72 Because of the observable, polarizing effects of the transverse field on large structures like

73 the cell body, it is reasonable to speculate that a transverse field could also play a significant role

74 in the polarization of axons. Indeed, evidence favoring transversal activation of axons also appear

75 in the literature. It was reported (Pourtaheri et al. 2009) that individual axons can be selectively

76 activated by a transverse field in a nerve bundle. These fields produce strong effects in the

77 stimulation of ulnar nerves (Cros et al. 1990; Olney et al. 1990) and long fibers (Grill & Wei 2009).

78 Using a magnetic coil to induce the electric field, Ruohonen et al. (Ruohonen et al. 1996)

79 discovered that activation of peripheral nerves could occur when the coil was oriented in a way

80 that only generated $E_\perp$, and a later theoretical work (Ye et al. 2011) confirmed the axonal

81 depolarization by this field. Clinically, the fast switching of magnetic fields during MRI scanning

82 generates $E_\perp$ in patients, which is considered an important risk factor for unwanted peripheral

83 nerve stimulation (While & Forbes 2004).

84 At present, the consensus is that $E_\perp$ is a modulator to the dominant effects caused by $E_{//}$,

85 although some researchers have speculated that the stimulation effects from transverse fields may

86 arise due to nerve undulation, which generates longitudinal field components (Lontis et al. 2009;

87 Schnabel & Struijk 1999; Struijk & Durand 1998). In the presence of $E_{//}$, it was thought that $E_\perp$

88 could introduce subthreshold membrane depolarization which enhances stimulation by providing

89 an additive effect on $E_{//}$ (Lontis et al. 2009). Alternatively, $E_{\perp}$ may provide rapid axonal

90 polarization in the transverse direction and $E_{//}$ drives the slow development of the mean

91 transmembrane potential (Cranford et al. 2012). $E_{//}$ and $E_{\perp}$ could potentially provide a strategy

92 for differential activation of axons with different properties (Ruohonen et al. 1996).

93 **Modify cable equation to include the contribution of transverse field**

94   In cases with significant transverse stimuli, where the membrane-field interaction is

95 sufficient and polarization is primarily due to the transverse field, the cable model assumptions are

96 known to be invalid (Krassowska & Neu 1994). Many modeling studies have argued for the

97 inclusion of the transverse field for the accurate simulation of neural activation, as well as the

98 development of mathematical tools to serve this purpose (Gimsa & Wachner 2001; Kotnik &

99 Miklavcic 2000a; Kotnik & Miklavcic 2006; Krassowska & Neu 1994; Ye et al. 2011; Ye &

100 Steiger 2015).

101   Several papers have reported their first endeavors for modifying the cable equation. Yu et

102 al. (Yu et al. 2005) modified the activation function to include the transversal field in magnetic

103 stimulation. Ravazzani et al. magnetically stimulated the median nerve and recorded the evoked

104 muscle responses, and discovered that including the transversal field in the cable equation provided

105 a much improved correlation between the mush EMG and the activating function (Ravazzani et al.

106 1996). A recent endeavor, which modified the current cable equation to include the transversal

107 term (Wang et al. 2018), showed that the transversal field could affect threshold of demyelinated

108 axons, but not in myelinated axons. Another work by the same group included the transverse term

109 in the cable equation that describes magnetic field stimulation (Wang 2018). In both these studies,

110 the membrane was represented by a resistor in parallel with a membrane capacitance. For

111 computational simplicity, all the above-mentioned works ignored the physical presence of the lipid

112 bilayer membrane, a "shell" like structure that has non-zero thickness. Consequently, the field

113 perturbation caused by the membrane, which is essential for the re-distribution of the transverse

114 field proximal to the axon (Farkas et al. 1984) (Jerry et al. 1996) (Lee & Grill 2005) (Mossop et

115 al. 2007), as well as the buildup of transmembrane potential (Kotnik & Miklavcic 2000a; Kotnik

116 & Miklavcic 2000b) through cell-field interaction (Ye & Steiger 2015), were ignored.

117 Furthermore, in the myelinated axon model, the possibility that the presence of the myelin sheath

118 might shield the internal structure such as the axon membrane (Kotnik & Miklavcic 2006; Ye &

119 Curcuru 2016) was not considered.

120   In the present paper, we model a bare axon as a conductive cylindrical shell, and provide
121   an analytical expression of membrane polarization (*Vm*) for an unmyelinated axon (or the node of
122   Ranvier in myelinated axon), under transverse electric field stimulation. We also provide *Vm* for
123   a myelin-covered axon, which was modeled as a co-centric, two shell structure. We investigate
124   biophysical factors that may affect the *Vm*, including field intensity and orientation, axonal
125   biophysics and the impact of pathological demyelination. We discuss the possibility of placing *Vm*
126   into a modified cable equation, so that the contributions of both the longitudinal and transverse
127   components of an electrical field could be simultaneously evaluated during electric stimulation of
128   axons.

129

130   **METHOD**

131   **Cylindrical axon model in a transverse electric field**

132   We modeled a bare axon and its myelin sheath using homogeneous cylindrical volume
133   conductors (Esselle & Stuchly 1994; Schnabel & Struijk 2001). Figure 1A illustrates the location and
134   orientation of a myelin-covered axon in a cylindrical coordinate system (r,θ,z). The axon was
135   exposed to a transverse, direct current (DC) electric field (E_0). It included a total of five isotropic and
136   homogenous regions: the medium (#0), the myelin sheath (#1), the periaxonal space (#2), the
137   axolemma (#3), and the axonal cytoplasm (#4). The dielectric permittivities and conductivities in the
138   five regions were $\varepsilon_0,\varepsilon_1,\varepsilon_2,\varepsilon_3,\varepsilon_4$ and $\sigma_0,\sigma_1,\sigma_2,\sigma_3,\sigma_4$, respectively. The myelin had an outer radius
139   (*a*), inner radius (*b*) and the thickness (*b-a*). The axon had an outer radius (*c*) and inner radius (*d*).
140   Thickness of the axolemma was therefore *c-d*. Figure 1B illustrates a bare axon, which was composed
141   of only the periaxonal space (#2), the axolemma (#3) and the axonal cytoplasm regions.

142   **Governing equation and boundary conditions**

143   Using the cylindrical coordinates (r,θ,z), the electric field distribution was calculated by

$$\mathbf{E} = -\nabla V = -(\frac{\partial V}{\partial r}, \frac{1}{r}\frac{\partial V}{\partial \theta}, \frac{\partial V}{\partial z}) \qquad (1)$$

145   For the DC electric field stimulation, an electric potential was obtained by solving Laplace's equation

$$\nabla^2 V = 0 \qquad\qquad (2)$$

147   The potential, V, is the electric scalar potential due to the charge accumulation between the interface

148   of the two different media (Stratton 1941). In a cylindrical coordinate system (r,θ,z), it is written as

149
$$\frac{1}{r}\frac{\partial}{\partial r}\left(r\frac{\partial V}{\partial r}\right) + \frac{1}{r^2}\frac{\partial^2 V}{\partial \theta^2} = 0 \qquad (3)$$

150   Several boundary conditions were evaluated in solving the equation (Appendix): (A). The

151   electric potential was continuous across the boundary of the two different media. (B). The normal

152   current density was continuous across the two different media. "Complex conductivity", defined as

153   $S = \sigma + j\omega\varepsilon$, was calculated to account for the dielectric permittivity of the material (Kotnik &

154   Miklavcic 2000b; Kotnik et al. 1998; Polk & Song 1990). Here, σ was the conductivity of the tissue,

155   ε was the permittivity, ω was the angular frequency of the field (zero for DC electric field) and

156   $j = \sqrt{-1}$ was the imaginary unit. On the extracellular media/myelin interface (#0#1, $r=a$),

157
$$S_0 E_{0r} - S_1 E_{1r} = 0 \qquad (4)$$

158   On the myelin /periaxonal interface (#1#2, $r=b$),

159
$$S_1 E_{1r} - S_2 E_{2r} = 0 \qquad (5)$$

160   On the periaxonal/axon interface (#2#3, $r=c$),

161
$$S_2 E_{2r} - S_3 E_{3r} = 0 \qquad (6)$$

162   On the axon/cytoplasm interface (#3#4, $r=d$),

163
$$S_3 E_{3r} - S_4 E_{4r} = 0 \qquad (7)$$

164   where $S_0 = \sigma_0 + j\omega\varepsilon_0, S_1 = \sigma_1 + j\omega\varepsilon_1, S_2 = \sigma_2 + j\omega\varepsilon_2, S_3 = \sigma_3 + j\omega\varepsilon_3, S_4 = \sigma_4 + j\omega\varepsilon_4$.   (C).

165   Electric fields an infinite distance away should not be perturbed by presence of the axon. (D). The

166   electric potential inside the cytoplasm ($r=0$) was finite.

167   **Model parameters**

168   Table 1 lists the default values of the model parameters and their ranges. The choice of the

169   electric parameters were based on reports in the literature (Kotnik et al. 1997; Kotnik & Miklavcic

170   2006). Axon radius was selected from Berthold and Rydmark (Berthold & Rydmark 1995). The

171   diameter of the unmyelinated axons ranges from approximately 0.1 μm to 2 μm (3 μm in humans).

172   We used 0.6 μm as the standard value and 0.1 – 3 μm as the range. The thickness of the axonal

173   membrane was selected from Nagarajan and Durant (Nagarajan & Durand 1995). The diameter of

174   the myelin was set to double the axon diameter. Lamella are produced by many layers of processes

175   from oligodendrocytes with significant membrane resistivity (Bakiri et al. 2011). The resistance of

176   the myelin was scaled linearly by the number (*n*) of lamella (Chomiak & Hu 2009). The standard

177   electric intensity was 200 V/m. The maximum intensity is the one that can cause membrane

178   electroporation (Sadik et al. 2011).

179   **Software packages**

180   Equations were derived with Mathematica 10 (Wolfram Research, Inc. Champaign, IL).

181   Numerical simulations were performed with Matlab 8.4.0 (The MathWorks, Inc. Natick, MA).

182

183   **RESULTS**

184   **Analytical expressions of axonal transmembrane potential (*Vm*) and voltage drop on the**

185   **myelin sheath (ϕ) under transverse electric stimulation**

186   The solution for Laplace's equation (Eq. 3) was written in the form (Griffiths 1999)

187    $V(r,\theta) = A_0 \ln(r) + B_0 +$

188    $\sum_{n=1}^{\infty} r^n [A_n \sin(n\theta) + B_n \cos(n\theta)] + \sum_{n=-\infty}^{-1} r^n [C_n \sin(n\theta) + D_n \cos(n\theta)]$ (8)

189   The expression was further simplified for the five modeled regions (Griffiths 1999; Ye et al. 2011)

190    $V_n = (\dfrac{A_n}{r} + C_n r) \sin \theta$ (9)

191   where A_n, C_n were unknown coefficients ($n = 0,1,2,3,4$). These coefficients were solved in the

192   Appendix (Supplementary file 1), by considering boundary conditions (A)-(D). Substituting A_3, C_3

193   into (9), we obtained the expression of voltage inside the axolemma

194    $V_3 = -\dfrac{8a^2 b^2 c^2 E_0 S_0 S_1 S_2 \cos\theta}{r} [\dfrac{term1}{term2 + term3}]$ (10)

195   Where

196    $term1 = d^2(S_3 - S_4) + r^2(S_3 + S_4)$

197    $term2 = b^2(S_0 - S_1) \times$

198 $\{c^2(S_1 + S_2)[d^2(S_2 + S_3)(S_3 - S_4) + c^2(S_2 - S_3)(S_3 + S_4)] + b^2(S_1 - S_2)[d^2(S_2 - S_3)(S_3 - S_4) + c^2(S_2 + S_3)(S_3 + S_4)]\}$

199 $term3 = a^2(S_0 + S_1)\times$

200 $$\{c^2(S_1 - S_2)[d^2(S_2 + S_3)(S_3 - S_4) + c^2(S_2 - S_3)(S_3 + S_4)] + b^2(S_1 + S_2) \\ [d^2(S_2 - S_3)(S_3 - S_4) + c^2(S_2 + S_3)(S_3 + S_4)]\}$$

201   The axonal transmembrane potential (Vm) of the field was obtained by subtracting

202 the membrane potential at the inner surface from that of the outer surface of the axon

203 (Kotnik et al. 1997; Kotnik & Miklavcic 2000a; Ye et al. 2011; Ye et al. 2010),

204 $V_m = V_3(r = d) - V_3(r = c)$. For a myelin-covered axon (Supplementary file 2),

205 $V_m = 8a^2b^2c(c - d)E_0S_0[\frac{term4}{term2 + term3}]\cos\theta$ (11)

206 Where

207 $term4 = S_1S_2[d(-S_3 + S_4) + c(S_3 + S_4)]$

208 Voltage drop (ϕ) across the myelin sheath was obtained by subtracting the myelin potential at the

209 inner surface from the outer surface of the myelin (Supplementary file 2)

210 $\emptyset = 2a(a - b)E_0S_0[\frac{term5 + term6}{term2 + term3}]\cos\theta$ (12)

211   Where

212 $term5 = b\{c^2(S_1 + S_2)\times$

213 $$[d^2(S_2 + S_3)(-S_3 + S_4) - c^2(S_2 - S_3)(S_3 + S_4)] - b^2(S_1 - S_2) \\ [d^2(S_2 - S_3)(S_3 - S_4) + c^2(S_2 + S_3)(S_3 + S_4)]\}$$

214 $term6 = a\{c^2(S_1 - S_2)\times$

215 $$[d^2(S_2 + S_3)(S_3 - S_4) + c^2(S_2 - S_3)(S_3 + S_4)] + b^2(S_1 + S_2) \\ [d^2(S_2 - S_3)(S_3 - S_4) + c^2(S_2 + S_3)(S_3 + S_4)]\}$$

216   Vm and ϕ were functions of both field properties and tissue properties. The field properties

217 included the orientation of the field and its intensity. The tissue properties include the electric

218   parameters (conductivity and di-electricity) and the geometrical parameters (i.e., diameters of the

219   axon). The above *Vm* expression for the myelin-covered axon (Eq. 11) was further simplified for

220   a bare axon by assuming $S_1 = S_0$ and $S_2 = S_0$ (Supplementary file 3),

221    $$V_m = \frac{2c(c-d)E_0 S_0[d(-S_3 + S_4) + c(S_3 + S_4)]}{d^2(S_0 - S_3)(S_3 - S_4) + c^2(S_0 + S_3)(S_3 + S_4)} cos\theta \qquad (13)$$

222   **Impact of electric field properties on *Vm***

223   When a transverse electric field penetrates the axolemma, the geometrical pattern of *Vm* is

224   determined by the axon's orientation to the electric field. The axolemma should be hyperpolarized

225   wherever an electric current enters the membrane and be depolarized wherever the current extrudes

226   from the membrane (Ye & Steiger 2015). We plotted the transmembrane potential for a 50 μm

227   myelinated axon (Figure 2A) and a straight bare axon (Figure 2B), based on the calculated *Vm*

228   using standard values (Table 1). As expected, the locations of maximum polarization were at two

229   lines corresponding to when θ=180° (hyperpolarization, blue) and θ = 0° (depolarization, yellow),

230   respectively. The axons were not polarized at the locations where θ= 90° and θ = 270°.

231   When the axon was wrapped by a thick myelin sheath, the geometrical pattern of the

232   axolemma depolarization (Figure 2A) remained identical to an unmyelinated axon (Figure 2B).

233   However, since a large voltage gradient (ϕ) was generated on the myelin sheath rather than on the

234   axolemma, *Vm* was quantitatively negligible for the myelinated axon. With the standard values in

235   Table 1, the maximum ϕ was 0.6 mV for the myelin sheath, and the maximum *Vm* was only

236   0.53×10^{-2} μV for the axolemma. In contrast, when the axon was not myelinated, the maximum

237   *Vm* was 0.24 mV.

238   For both the myelin-covered and bare axons, *Vm* was proportional to the intensity of the

239   electric field (Figures 2C and 2D). 2 kV/cm was sufficient in inducing electroporation (Sadik et

240   al. 2011). This intensity induced a *Vm* of 5.3 μV for the myelin-covered axon. For a bare axon, it

241   induced a *Vm* of 239.9 mV, which is sufficient to break down the structure of the membrane (Gehl

242   2003; Kinosita & Tsong 1977). These results suggest that the myelin sheath could provide a

243   "shielding effect" on the axolemma against field-induced excessive polarization and structure

244   disruption.

245   **Impact of axonal properties on *Vm***

246   We investigated the dependency of *Vm* on the axonal properties, including the geometrical

247   features (axon radius and membrane thickness) of the axon, and its conductivity. For the

248   parametric analysis, we plotted the maximum polarization ($\theta = 0^0$ on the axon surface, Figures 1

249   and 2) when one parameter was varied through its defined value range, while the others were

250   maintained at their standard values.

251   An axon with a larger radius was associated with a greater *Vm* for both the myelin-covered

252   axon and bare axon (Figure 3A) under a transverse field stimulation. Axon thickness, however,

253   did not significantly affect *Vm* (Figure 3B). *Vm* was insensitive to the axonal conductance changes

254   within its physiological range (10^{-8}-10^{-6} S/m), in agreement with the literature that studied

255   spherical cell polarization in an electric field (Kotnik et al. 1997; Kotnik & Miklavcic 2006).

256   However, when axolemma conductivity was significantly increased (>10^{-3} S/m) due to membrane

257   disruption and leakage, such as during electroporation (Mossop et al. 2007; Mossop et al. 2004),

258   axolemma depolarization decreased significantly for both the myelin-covered and bare axons

259   (Figure 3C).

260

261   Impact of demyelination on axonal *Vm*

262   Myelin, like a neuronal cell membrane, is constructed of a lipid bilayer that contains a

263   hydrophobic center and hydrophilic surface. Myelin wraps around an axon numerous times, each

264   layer acting like multiple resistors in series. Demyelination occurs in many neurological diseases

265   such as spinal cord injury (Ye et al. 2012), cerebral palsy (Ruff et al. 2013) and multiple sclerosis

266   (Lazzarini 2004). Demyelination is defined by the significant loss of myelin thickness (Mainero

267   et al. 2015; Manogaran et al. 2016) and increased conductivity of the myelin.

268   We first studied how the loss of myelin layers could affect *Vm* in a transverse electric field.

269   We systematically decreased the myelin thickness from 4.0 μm to 0.1 μm. The conductivity of the

270   myelin increased linearly with the reduction of the myelin thickness. This caused a reduction in

271   the potential drop across the myelin sheath, but it did not significantly affect axonal depolarization

272   (Figure 4). The transverse electric field was ineffective in inducing axonal depolarization,

273   assuming the remaining myelin sheath could maintain low conductivity (~10^{-7} S/m).

274   We then investigated how an increase of myelin conductivity could affect *Vm* in a

275   transverse electric field. When myelin conductivity was as low as 5×10^{-5} S/m, reduction in myelin

276   thickness did not lead to dramatic changes in *Vm* (Figure 5A). Instead, it led to a voltage drop

277   across the myelin sheath (ϕ). When myelin conductivity was increased to 5×10^{-3} S/m, *Vm* could

278   exceed ϕ for an extremely thin myelin sheath (Figure 5B). For a very leaky myelin (myelin

279   conductivity is 5×10^{-1} S/m), the axon could be significantly depolarized at any myelin thickness

280   (Figure 5C), and *Vm* could be greater than ϕ for a thin myelin sheath (Figure 5C, left inset).

281   However, ϕ still dominated for axons with thick myelin sheaths (Figure 5C, right inset). In

282   conclusion, demyelination could cause a re-distribution of the potentials between the axolemma

283   and myelin under transverse electric stimulation. Increases in myelin conductivity during

284   demyelination could cause the voltage distribution to shift from the myelin sheath to the axon.

285   Axonal depolarization became prominent when significant reduction of myelin conductivity

286   occurred during demyelination.

287   **DISCUSSION**

288   This work provides a novel analytical expression that describes the membrane polarization

289   of axons (myelinated and bare) under transverse field stimulation. It analyzes the biophysical

290   factors that affect axonal polarization under physiological conditions, and under pathological

291   conditions such as demyelination. Finally, it provides the needed term to modify the current cable

292   equation, so that the equation can account for the effects of more realistic field, which include both

293   the transverse and parallel directions.

294   **Impact of field orientation on *Vm* in transverse current stimulation**

295   The model shows that the longitudinal axon was polarized with a distinct geometrical

296   pattern by the transverse electric field, which was dependent on the orientation of the axon in the

297   field. Previously, regional polarization has been observed in a variety of modeling and

298   experimental studies for cells under electric (Durand 2003; Lee & Grill 2005; Lu et al. 2008; Teruel

299   & Meyer 1997) and magnetic field stimulation (Schnabel & Struijk 1999; Schnabel & Struijk

300   2001; Ye et al. 2007). Functionally, orientation of the electric field to the axon is important for the

301   excitation of axons, such as those from the retina ganglion cells (Grumet et al. 2000). Since only

302   a small patch of membrane is depolarized in the transverse field, it is reasonable to speculate that

303   voltage gated ion channels may have a diverse response to the field, depending on their location

304   on the membrane patch. This could cause the threshold for activation to be higher than that

305   observed from axons in longitudinal fields that induce the same peak depolarization (Schnabel &

306   Struijk 2001). The higher threshold may explain the relative poor efficiency of axonal activation

307   by transverse field stimulation (McNeal 1976; Ranck 1975).

308   Impact of axon's biophysical properties on Vm

309   We found that Vm was dependent on the intrinsic tissue properties of an axon. We observed

310   that Vm was greater in larger diameter axons than in smaller ones (Figure 3A). This observation

311   is in agreement with the notion that larger diameter axons are associated with lower excitation

312   thresholds (Basser & Roth 1991; Carbunaru & Durand 1997; Garnsworthy et al. 1988; Reilly

313   1989). Selective activation of different size fibers has significant clinical implications, such as pain

314   relief (Meyerson & Linderoth 2000), which can be achieved by novel design of the electric field

315   (Konings 2007). In deep brain stimulation (DBS), the effects of the electric currents within

316   different brain regions were dependent on the fiber sizes (Sotiropoulos & Steinmetz 2007). In

317   addition, an increase in axolemma conductivity decreases the axon's sensitivity (buildup of Vm)

318   to the transverse field (Figure 3C), suggesting a shunting effect to the transverse current. In

319   conclusion, the effectiveness of transverse stimulation relies on the physiological features of the

320   target axon.

321   Axonal diameter could change under certain pathological situations. For example, axon

322   swelling occurs during focal demyelination (Kolaric et al. 2013), as a consequence of aglycemia

323   (Allen et al. 2006), anoxia (Waxman et al. 1992) or ischemia (Garthwaite et al. 1999). It is

324   speculated that these pathological changes could potentially render the enlarged axons more

325   sensitive to the transverse electric field.

326

327   Impact of demyelination and other pathological conditions on Vm in transverse electric

328   stimulation

329   Dynamic changes of myelin occur during demyelination. It is unknown if pathological

330   demyelination could affect the sensitivity of a myelinated axon to a transverse electric field. While

331   myelin-covered axons could only be slightly depolarized by the transverse field, bare axons can

332   have a moderate buildup of Vm (Figure 2), especially when the axon diameter is large (Figure 5A).

333   We used the model to test two possibilities of reduced myelination and their impacts on Vm.

334   Reduction in the myelin thickness, along with a scaled linear increase in myelin conductance, was

335   not sufficient to enhance depolarization (Figure 4). In contrast, Vm was enhanced when the myelin

336   sheath became electrically leaky (highly conductive) (Figure 5). It is therefore expected that

337   transverse electric fields could apply variable axonal depolarization, depending on the myelin

338   conductivity changes during the process of demyelination. Electrical stimulation protocols for the

339   treatment of demyelination diseases (Dooley & Sharkey 1981; Dooley et al. 1978) could be further

340   optimized by considering remyelination/demyelination factors during treatment, to ensure

341   maximum outcomes.

342   Dynamic changes of myelin also occur during development (Sturrock 1980), neural

343   regeneration (Huang et al. 2013), and pathological situations such as traumatic brain injury

344   (Robain & Mandel 1974; Tyler 2012). At the cellular level, membrane resistance of the

345   oligodendrocyte could change during development and maturity (Karadottir et al. 2005), and in a

346   medium with low osmolarity (Kimelberg & Kettenmann 1990). It is speculated that these dynamic

347   changes in the myelin properties could cause the axons to react differently to the electric field.

348   This supports the notion that the dynamic interaction between the electric field and the neuronal

349   tissue, as well as the outcome of the stimulation, are determined by both the electric parameters

350   and the tissue properties (Ye & Steiger 2015).

351   **Modification of the cable equation to include the transverse field**

352   The analytical expression of the *Vm* term could potentially be used to modify the current

353   cable equation to account for both $E_{//}$ and $E_{\perp}$. Ruohonen et al. modified the cable equation

354   (Ruohonen et al. 1996) to be in the form of $\lambda^2 \dfrac{\partial^2 \varphi_m}{\partial x^2} - \tau \dfrac{\partial \varphi_m}{\partial t} - \varphi_m - 2c(\alpha E_{//}' - E_{\perp}) = 0$. Here,

355   $\alpha E_{//}' - E_{\perp}$ is interpreted as the *modified activating function*, where $\alpha = \dfrac{\lambda^2}{2c} = \dfrac{R_m}{4R_i}$ (Ruohonen et al.

356   1996). Comparatively large values of α indicates that $E_{//}'$ is responsible for the majority of

357   excitation, while $\alpha = 0$ indicates that $E_{\perp}$ is more important.

358   In this modified equation, the term $2cE_{\perp}$ is the membrane potential created by the

359   transverse field. For magnetic stimulation, an analytical expression (Ye et al. 2011) is available

360   to replace this term for the modified cable equation. For direct electric stimulation, the *Vm* term

361   for the unmyelinated axon (Eq. 13) can be used to replace the $2cE_{\perp}$ term, to include the impact of

362   the transverse electric field. Previously, effects of the transverse field and the axial field have been

363   compared in several works (Lontis et al. 2009; Ruohonen et al. 1996; Yu et al. 2005). The

364 transverse electric field is required to be several times greater than the longitudinal field to produce
365 comparable results (McNeal 1976; Ranck 1975; Ruohonen et al. 1996). A precondition for the
366 modified activation function to yield accurate results is for the electric field to be approximately
367 uniform and be perpendicular to the axon fiber (Schnabel & Struijk 2001), which is readily
368 satisfied in our model.

369

370 **Limitations and future directions**

371 This paper was not intended to fully elucidate the mechanisms behind transverse field
372 activation of nerve tissue, since it did not include any ionic channel mechanisms. The model also
373 does not necessarily apply to the stimulation of fiber bundles. Axons within a bundle could
374 interfere with other axon's polarization under a transverse electric field (Pourtaheri et al. 2009).
375 Local electric fields could be perturbed by an axon, which produces a small, secondary effect on
376 the surrounding axons (Lee & Grill 2005; Susil et al. 1998). In a nerve bundle, Vm could also be
377 a function of the anisotropy of the bundle (Nagarajan & Durand 1995), which was not studied in
378 the present model. Finally, the transverse field could be significantly weaker due to the lower
379 values of conductance of surrounding perineurium (Struijk & Schnabel 2001). More complicated
380 modeling work should resort to numerical methods, whose accuracy can be validated by the
381 analytical results from this work.

382 The model predicts that the node section in a myelinated axon will have the same
383 polarization as the unmyelinated axon. If one considers that the node has a much higher density of
384 Na^+ channel distribution (Freeman et al. 2016), it is predicted that myelinated axons will have a
385 lower threshold of activation under transverse electric field. This model prediction could be tested
386 by stimulating a structure that contains both unmyelinated and myelinated axons, such as the
387 corpus callosum (Crawford et al. 2009; Ruff et al. 2013). With the strong stimulus being applied
388 on both type of axons (Ruff et al. 2013), action potentials should be triggered first in the myelinated
389 axons.

390 **Conclusions**

391 This work provides novel analytical expressions of the electrically-induced transmembrane
392 potential ($Vm)$ for a myelin-covered axon and a bare, unmyelinated axon, under a transverse DC
393 electric field. Results show that the myelin sheath shields the axon from extensive depolarization.

394 Demyelination could alter axon's sensitivity to a transverse electric field if the process of

395 demyelination involves significant increases in the electric conductance of the myelin. The

396 analytical solution of *Vm* for the unmyelinated axon can be used to improve the activation function

397 of the current cable equation that describes electric stimulation.

398

399 Acknowledgements:

400   The authors thanks Austen Curcuru for the assistance in deriving the equations.

401

402 **Appendix - Determining unknown coefficients** A_n, C_n **in equation (9) using boundary**

403 **conditions (A)-(D)**

404   At an infinite distance, according to boundary condition (C), $V_o = -E_0 r \cos\theta$. Therefore,

405 $a_0 = -E_0$. Since V was bounded at $r = 0$ (boundary condition D), $C_4 = 0$.

406 Expressions for the potential distribution in the five modeled regions were:

407 $V_0 = -E_0 r \cos\theta + \dfrac{C_0}{r} \cos\theta \quad$ (A-1)

408 $V_1 = A_1 r \cos\theta + \dfrac{C_1}{r} \cos\theta \quad$ (A-2)

409 $V_2 = A_2 r \cos\theta + \dfrac{C_2}{r} \cos\theta \quad$ (A-3)

410 $V_3 = A_3 r \cos\theta + \dfrac{C_3}{r} \cos\theta \quad$ (A-4)

411 $V_4 = A_4 r \cos\theta \quad$ (A-5)

412 The $\breve{r}$ components of ∇V (from Eq. 1) were continuous across the interfaces (boundary condition

413 A), and the normal components of the current density were continuous across the interfaces

414 (boundary condition B). These boundary conditions yield the following set of equations:

415   On the #0#1 interface (r=a)

416    $-E_0 a + \dfrac{C_0}{a} = aA_1 + \dfrac{C_1}{a}$ (A-6)

417    $S_0(-E_0 - \dfrac{C_0}{a^2} = S_1(A_1 - \dfrac{C_{11}}{a^2})$ (A-7)

418   On the #1#2 interface (r=b)

419    $bA_1 + \dfrac{C_1}{b} = bA_2 + \dfrac{C_2}{b}$ (A-8)

420    $S_1(A_1 - \dfrac{C_1}{b^2}) = S_2(A_2 - \dfrac{C_2}{b^2})$ (A-9)

421   On the #2#3 interface (r=c)

422    $cA_2 + \dfrac{C_2}{c} = cA_3 + \dfrac{C_3}{c}$ (A-10)

423    $S_2(A_2 - \dfrac{C_2}{c^2}) = S_3(A_3 - \dfrac{C_3}{c^2})$ (A-11)

424   On the #3#4 interface (r=d)

425    $dA_3 + \dfrac{C_3}{d} = dA_4$ (A-12)

426    $S_3(A_3 - \dfrac{C_3}{d^2}) = S_4 A_4$ (A-13)

427   We solved (A-6) to (A-13) to obtain the unknown coefficients (Supplementary file 1). These

428   coefficients will be substituted into (A-1) to (A-5) to obtain the analytical expression of the

429   voltages in the five regions (Supplementary file 1).

430   **List of Abbreviations**

431   DC: Direct current; E_0: Intensity of the externally applied DC electric field (V/m); Vm:

432   Transmembrane potential induced by the DC electric field across the axolemma (mV); ϕ: Potential

433   drop across the myelin sheath (mV); $E_{//}$: Electric field that is parallel to the axon; $E_{\perp}$: Electric

434   field that is perpendicular (traversal) to the axon.

References

436   Allen L, Anderson S, Wender R, Meakin P, Ransom BR, Ray DE, and Brown AM. 2006. Fructose supports
437   energy metabolism of some, but not all, axons in adult mouse optic nerve. *J Neurophysiol*
438   95:1917-1925. 10.1152/jn.00637.2005
439   Amassian VE, Maccabee PJ, and Cracco RQ. 1989. Focal stimulation of human peripheral nerve with the
440   magnetic coil: a comparison with electrical stimulation. *Exp Neurol* 103:282-289.
441   Bakiri Y, Karadottir R, Cossell L, and Attwell D. 2011. Morphological and electrical properties of
442   oligodendrocytes in the white matter of the corpus callosum and cerebellum. *J Physiol* 589:559-
443   573. 10.1113/jphysiol.2010.201376
444   Basser PJ, and Roth BJ. 1991. Stimulation of a myelinated nerve axon by electromagnetic induction. *Med*
445   *Biol Eng Comput* 29:261-268.
446   Basser PJ, and Roth BJ. 2000. New currents in electrical stimulation of excitable tissues. *Annu Rev*
447   *Biomed Eng* 2:377-397. 10.1146/annurev.bioeng.2.1.377
448   Basser PJ, Wijesinghe RS, and Roth BJ. 1992. The activating function for magnetic stimulation derived
449   from a three-dimensional volume conductor model. *IEEE Trans Biomed Eng* 39:1207-1210.
450   10.1109/10.168686
451   Berthold CH, and Rydmark M. 1995. Morphology of Normal Peripheral Axon. In: Waxman SG, Kocsis JD,
452   and Stys PK, eds. *The Axon: Structure, Function, and Pathophysiology*: Oxford University Press
453   US.
454   Bikson M, Lian J, Hahn PJ, Stacey WC, Sciortino C, and Durand DM. 2001. Suppression of epileptiform
455   activity by high frequency sinusoidal fields in rat hippocampal slices. *J Physiol* 531:181-191.
456   Bingham RJ, Olmsted PD, and Smye SW. 2010. Undulation instability in a bilayer lipid membrane due to
457   electric field interaction with lipid dipoles. *Phys Rev E Stat Nonlin Soft Matter Phys* 81:051909.
458   10.1103/PhysRevE.81.051909
459   Carbunaru R, and Durand DM. 1997. Axonal stimulation under MRI magnetic field z gradients: a
460   modeling study. *Magn Reson Med* 38:750-758.
461   Chomiak T, and Hu B. 2009. What is the optimal value of the g-ratio for myelinated fibers in the rat CNS?
462   A theoretical approach. *PLoS One* 4:e7754. 10.1371/journal.pone.0007754
463   Coderre TJ, Katz J, Vaccarino AL, and Melzack R. 1993. Contribution of central neuroplasticity to
464   pathological pain: review of clinical and experimental evidence. *Pain* 52:259-285.
465   Cranford JP, Kim BJ, and Neu WK. 2012. Asymptotic model of electrical stimulation of nerve fibers. *Med*
466   *Biol Eng Comput* 50:243-251. 10.1007/s11517-012-0870-3
467   Crawford DK, Mangiardi M, and Tiwari-Woodruff SK. 2009. Assaying the functional effects of
468   demyelination and remyelination: revisiting field potential recordings. *J Neurosci Methods*
469   182:25-33. 10.1016/j.jneumeth.2009.05.013
470   Cros D, Day TJ, and Shahani BT. 1990. Spatial dispersion of magnetic stimulation in peripheral nerves.
471   *Muscle Nerve* 13:1076-1082. 10.1002/mus.880131110
472   Dooley DM, and Sharkey J. 1981. Electrical stimulation of the spinal cord in patients with demyelinating
473   and degenerative diseases of the central nervous system. *Appl Neurophysiol* 44:218-224.
474   Dooley DM, Sharkey J, Keller W, and Kasprak M. 1978. Treatment of demyelinating and degenerative
475   diseases by electro stimulation of the spinal cord. *Med Prog Technol* 6:1-14.
476   Durand DM. 2003. Electric field effects in hyperexcitable neural tissue: a review. *Radiat Prot Dosimetry*
477   106:325-331.

478 Esselle KP, and Stuchly MA. 1994. Quasi-static electric field in a cylindrical volume conductor induced by
479   external coils. *IEEE Trans Biomed Eng* 41:151-158. 10.1109/10.284926
480 Esselle KP, and Stuchly MA. 1995. Cylindrical tissue model for magnetic field stimulation of neurons:
481   effects of coil geometry. *IEEE Trans Biomed Eng* 42:934-941. 10.1109/10.412660
482 Farkas DL, Korenstein R, and Malkin S. 1984. Electrophotoluminescence and the electrical properties of
483   the photosynthetic membrane. I. Initial kinetics and the charging capacitance of the membrane.
484   *Biophys J* 45:363-373. 10.1016/S0006-3495(84)84160-0
485 Freeman SA, Desmazieres A, Fricker D, Lubetzki C, and Sol-Foulon N. 2016. Mechanisms of sodium
486   channel clustering and its influence on axonal impulse conduction. *Cell Mol Life Sci* 73:723-735.
487   10.1007/s00018-015-2081-1
488 Fricke H. 1953. The Electric Permittivity of a Dilute Suspension of Membrane-Covered Ellipsoids. *J Appl*
489   *Phys* 24:644-646.
490 Galvani A. 1791. De viribus electricitatis in motu musculari commentaries. *Opuscula*:363-418.
491 Garnsworthy RK, Gully RL, Kenins P, and Westerman RA. 1988. Transcutaneous electrical stimulation and
492   the sensation of prickle. *J Neurophysiol* 59:1116-1127.
493 Garthwaite G, Brown G, Batchelor AM, Goodwin DA, and Garthwaite J. 1999. Mechanisms of ischaemic
494   damage to central white matter axons: a quantitative histological analysis using rat optic nerve.
495   *Neuroscience* 94:1219-1230.
496 Gehl J. 2003. Electroporation: theory and methods, perspectives for drug delivery, gene therapy and
497   research. *Acta Physiol Scand* 177:437-447. 10.1046/j.1365-201X.2003.01093.x
498 Gimsa J, and Wachner D. 2001. Analytical description of the transmembrane voltage induced on
499   arbitrarily oriented ellipsoidal and cylindrical cells. *Biophys J* 81:1888-1896. 10.1016/S0006-
500   3495(01)75840-7
501 Griffiths DJ. 1999. *Introduction to Electrodynamics. 3rd Edition*: Prentice Hall.
502 Grill WM, and Wei XF. 2009. High efficiency electrodes for deep brain stimulation. *Conf Proc IEEE Eng*
503   *Med Biol Soc* 2009:3298-3301. 10.1109/IEMBS.2009.5333774
504 Grumet AE, Wyatt JL, Jr., and Rizzo JF, 3rd. 2000. Multi-electrode stimulation and recording in the
505   isolated retina. *J Neurosci Methods* 101:31-42. S0165-0270(00)00246-6
506 Huang J, Zhang Y, Lu L, Hu X, and Luo Z. 2013. Electrical stimulation accelerates nerve regeneration and
507   functional recovery in delayed peripheral nerve injury in rats. *Eur J Neurosci* 38:3691-3701.
508   10.1111/ejn.12370
509 Jerry RA, Popel AS, and Brownell WE. 1996. Potential distribution for a spheroidal cell having a
510   conductive membrane in an electric field. *IEEE Trans Biomed Eng* 43:970-972.
511   10.1109/10.532132
512 Karadottir R, Cavelier P, Bergersen LH, and Attwell D. 2005. NMDA receptors are expressed in
513   oligodendrocytes and activated in ischaemia. *Nature* 438:1162-1166. 10.1038/nature04302
514 Kimelberg HK, and Kettenmann H. 1990. Swelling-induced changes in electrophysiological properties of
515   cultured astrocytes and oligodendrocytes. I. Effects on membrane potentials, input impedance
516   and cell-cell coupling. *Brain Res* 529:255-261.
517 Kinosita K, Jr., and Tsong TY. 1977. Voltage-induced pore formation and hemolysis of human
518   erythrocytes. *Biochim Biophys Acta* 471:227-242.
519 Kolaric KV, Thomson G, Edgar JM, and Brown AM. 2013. Focal axonal swellings and associated
520   ultrastructural changes attenuate conduction velocity in central nervous system axons: a
521   computer modeling study. *Physiol Rep* 1:e00059. 10.1002/phy2.59
522 Konings MK. 2007. A new method for spatially selective, non-invasive activation of neurons: concept and
523   computer simulation. *Med Biol Eng Comput* 45:7-24. 10.1007/s11517-006-0136-z
524 Kotnik T, Bobanovic F, and Miklavcic D. 1997. Sensitivity of Transmembrane Voltage Induced by Applied
525   Electric Fields—A Theoretical Analysis. *Bioelectrochem Bioenerg* 43:285-291.

526   Kotnik T, and Miklavcic D. 2000a. Analytical description of transmembrane voltage induced by electric
527   fields on spheroidal cells. *Biophys J* 79:670-679. 10.1016/S0006-3495(00)76325-9
528   Kotnik T, and Miklavcic D. 2000b. Second-order model of membrane electric field induced by alternating
529   external electric fields. *IEEE Trans Biomed Eng* 47:1074-1081. 10.1109/10.855935
530   Kotnik T, and Miklavcic D. 2006. Theoretical evaluation of voltage inducement on internal membranes of
531   biological cells exposed to electric fields. *Biophys J* 90:480-491. 10.1529/biophysj.105.070771
532   Kotnik T, Miklavcic D, and Slivnik T. 1998. Time course of transmembrane voltage induced by time-
533   varying electric field - a method for theoretical analysis and its application. *Bioelectrochem*
534   *Bioenerg* 45:3-16.
535   Krassowska W, and Neu JC. 1994. Response of a single cell to an external electric field. *Biophys J*
536   66:1768-1776. 10.1016/S0006-3495(94)80971-3
537   Lazzarini RA. 2004. *Myelin biology and disorders*. San Diego: Elsevier Academic.
538   Lee DC, and Grill WM. 2005. Polarization of a spherical cell in a nonuniform extracellular electric field.
539   *Ann Biomed Eng* 33:603-615.
540   Lontis ER, Nielsen K, and Struijk JJ. 2009. In vitro magnetic stimulation of pig phrenic nerve with
541   transverse and longitudinal induced electric fields: analysis of the stimulation site. *IEEE Trans*
542   *Biomed Eng* 56:500-512. 10.1109/TBME.2008.2009929
543   Lu H, Chestek CA, Shaw KM, and Chiel HJ. 2008. Selective extracellular stimulation of individual neurons
544   in ganglia. *J Neural Eng* 5:287-309. 10.1088/1741-2560/5/3/003
545   Maccabee PJ, Amassian VE, Cracco RQ, Eberle LP, and Rudell AP. 1991. Mechanisms of peripheral
546   nervous system stimulation using the magnetic coil. *Electroencephalogr Clin Neurophysiol Suppl*
547   43:344-361.
548   Maccabee PJ, Amassian VE, Eberle LP, and Cracco RQ. 1993. Magnetic coil stimulation of straight and
549   bent amphibian and mammalian peripheral nerve in vitro: locus of excitation. *J Physiol* 460:201-
550   219.
551   Mainero C, Louapre C, Govindarajan ST, Gianni C, Nielsen AS, Cohen-Adad J, Sloane J, and Kinkel RP.
552   2015. A gradient in cortical pathology in multiple sclerosis by in vivo quantitative 7 T imaging.
553   *Brain* 138:932-945. 10.1093/brain/awv011
554   Manogaran P, Vavasour IM, Lange AP, Zhao Y, McMullen K, Rauscher A, Carruthers R, Li DK, Traboulsee
555   AL, and Kolind SH. 2016. Quantifying visual pathway axonal and myelin loss in multiple sclerosis
556   and neuromyelitis optica. *Neuroimage Clin* 11:743-750. 10.1016/j.nicl.2016.05.014
557   McNeal DR. 1976. Analysis of a model for excitation of myelinated nerve. *IEEE Trans Biomed Eng* 23:329-
558   337.
559   Meyerson BA, and Linderoth B. 2000. Mechanisms of spinal cord stimulation in neuropathic pain. *Neurol*
560   *Res* 22:285-292.
561   Mossop BJ, Barr RC, Henshaw JW, and Yuan F. 2007. Electric fields around and within single cells during
562   electroporation-a model study. *Ann Biomed Eng* 35:1264-1275. 10.1007/s10439-007-9282-1
563   Mossop BJ, Barr RC, Zaharoff DA, and Yuan F. 2004. Electric fields within cells as a function of membrane
564   resistivity--a model study. *IEEE Trans Nanobioscience* 3:225-231.
565   Nagarajan SS, and Durand DM. 1995. Analysis of magnetic stimulation of a concentric axon in a nerve
566   bundle. *IEEE Trans Biomed Eng* 42:926-933. 10.1109/10.412659
567   Nowak LG, and Bullier J. 1998. Axons, but not cell bodies, are activated by electrical stimulation in
568   cortical gray matter. I. Evidence from chronaxie measurements. *Exp Brain Res* 118:477-488.
569   Olney RK, So YT, Goodin DS, and Aminoff MJ. 1990. A comparison of magnetic and electrical stimulation
570   of peripheral nerves. *Muscle Nerve* 13:957-963. 10.1002/mus.880131012
571   Polk C, and Song JH. 1990. Electric fields induced by low frequency magnetic fields in inhomogeneous
572   biological structures that are surrounded by an electric insulator. *Bioelectromagnetics* 11:235-
573   249.

574   Pourtaheri N, Ying W, Kim JM, and Henriquez CS. 2009. Thresholds for transverse stimulation: fiber
575   bundles in a uniform field. *IEEE Trans Neural Syst Rehabil Eng* 17:478-486.
576   10.1109/TNSRE.2009.2033424

577   Ranck JB, Jr. 1975. Which elements are excited in electrical stimulation of mammalian central nervous
578   system: a review. *Brain Res* 98:417-440.

579   Ravazzani P, Ruohonen J, Grandori F, and Tognola G. 1996. Magnetic stimulation of the nervous system:
580   induced electric field in unbounded, semi-infinite, spherical, and cylindrical media. *Ann Biomed*
581   *Eng* 24:606-616.

582   Reilly JP. 1989. Peripheral nerve stimulation by induced electric currents: exposure to time-varying
583   magnetic fields. *Med Biol Eng Comput* 27:101-110.

584   Robain O, and Mandel P. 1974. [Quantitative study of myelination and axonal growth in corpus callosum
585   and posterior columns of spinal cord in the Jimpy mouse (author's transl)]. *Acta Neuropathol*
586   29:293-309.

587   Roth BJ, and Basser PJ. 1990. A model of the stimulation of a nerve fiber by electromagnetic induction.
588   *IEEE Trans Biomed Eng* 37:588-597. 10.1109/10.55662

589   Roth BJ, Cohen LG, Hallett M, Friauf W, and Basser PJ. 1990. A theoretical calculation of the electric field
590   induced by magnetic stimulation of a peripheral nerve. *Muscle Nerve* 13:734-741.
591   10.1002/mus.880130812

592   Ruff CA, Ye H, Legasto JM, Stribbell NA, Wang J, Zhang L, and Fehlings MG. 2013. Effects of adult neural
593   precursor-derived myelination on axonal function in the perinatal congenitally dysmyelinated
594   brain: optimizing time of intervention, developing accurate prediction models, and enhancing
595   performance. *J Neurosci* 33:11899-11915. 10.1523/JNEUROSCI.1131-13.2013

596   Ruohonen J, Panizza M, Nilsson J, Ravazzani P, Grandori F, and Tognola G. 1996. Transverse-field
597   activation mechanism in magnetic stimulation of peripheral nerves. *Electroencephalogr Clin*
598   *Neurophysiol* 101:167-174.

599   Sadik MM, Li J, Shan JW, Shreiber DI, and Lin H. 2011. Vesicle deformation and poration under strong dc
600   electric fields. *Phys Rev E Stat Nonlin Soft Matter Phys* 83:066316.

601   Schnabel V, and Struijk JJ. 1999. Magnetic and electrical stimulation of undulating nerve fibres: a
602   simulation study. *Med Biol Eng Comput* 37:704-709.

603   Schnabel V, and Struijk JJ. 2001. Evaluation of the cable model for electrical stimulation of unmyelinated
604   nerve fibers. *IEEE Trans Biomed Eng* 48:1027-1033.

605   Schwan HP. 1957. Electrical properties of tissue and cell suspensions. *Adv Biol Med Phys* 5:147-209.

606   Selimbeyoglu A, and Parvizi J. 2010. Electrical stimulation of the human brain: perceptual and behavioral
607   phenomena reported in the old and new literature. *Front Hum Neurosci* 4:46.
608   10.3389/fnhum.2010.00046

609   Sotiropoulos SN, and Steinmetz PN. 2007. Assessing the direct effects of deep brain stimulation using
610   embedded axon models. *J Neural Eng* 4:107-119. 10.1088/1741-2560/4/2/011

611   Stratton J. 1941. *Electromagnetic Theory*. New York: McGraw-Hill.

612   Struijk JJ, and Durand DM. 1998. Magnetic peripheral nerve stimulation: axial verses transverse fields.
613   *Proceedings BMES/EMBS*. Atlanta, 469.

614   Struijk JJ, and Schnabel V. 2001. Difference between electrical and magnetic nerve stimulation: A case
615   for transverse field. *Proceedings of the 23rd Annual International Conference of IEEE*, 885-887.

616   Sturrock RR. 1980. Myelination of the mouse corpus callosum. *Neuropathol Appl Neurobiol* 6:415-420.

617   Susil R, Semrov D, and Miklavcic D. 1998. Electric field induced transmembrane potential depends on
618   cell density and organization. *Electro Magnetobiol* 17:391-399.

619   Teruel MN, and Meyer T. 1997. Electroporation-induced formation of individual calcium entry sites in
620   the cell body and processes of adherent cells. *Biophys J* 73:1785-1796. 10.1016/S0006-
621   3495(97)78209-2

622 Tyler WJ. 2012. The mechanobiology of brain function. *Nat Rev Neurosci* 13:867-878. 10.1038/nrn3383
623 Wang B, Aberra AS, Grill WM, and Peterchev AV. 2018. Modified cable equation incorporating
624   transverse polarization of neuronal membranes for accurate coupling of electric fields. *J Neural*
625   *Eng* 15:026003. 10.1088/1741-2552/aa8b7c
626 Waxman SG, Black JA, Stys PK, and Ransom BR. 1992. Ultrastructural concomitants of anoxic injury and
627   early post-anoxic recovery in rat optic nerve. *Brain Res* 574:105-119.
628 While PT, and Forbes LK. 2004. Electromagnetic fields in the human body due to switched transverse
629   gradient coils in MRI. *Phys Med Biol* 49:2779-2798.
630 Ye H, Buttigieg J, Wan Y, Wang J, Figley S, and Fehlings MG. 2012. Expression and functional role of BK
631   channels in chronically injured spinal cord white matter. *Neurobiol Dis* 47:225-236.
632   10.1016/j.nbd.2012.04.006
633 Ye H, Cotic M, and Carlen PL. 2007. Transmembrane potential induced in a spherical cell model under
634   low-frequency magnetic stimulation. *J Neural Eng* 4:283-293. 10.1088/1741-2560/4/3/014
635 Ye H, Cotic M, Fehlings MG, and Carlen PL. 2011. Transmembrane potential generated by a magnetically
636   induced transverse electric field in a cylindrical axonal model. *Med Biol Eng Comput* 49:107-119.
637   10.1007/s11517-010-0704-0
638 Ye H, Cotic M, Kang EE, Fehlings MG, and Carlen PL. 2010. Transmembrane potential induced on the
639   internal organelle by a time-varying magnetic field: a model study. *J Neuroeng Rehabil* 7:12.
640   10.1186/1743-0003-7-12
641 Ye H, and Curcuru A. 2016. Biomechanics of cell membrane under low-frequency time-varying magnetic
642   field: a shell model. *Med Biol Eng Comput* 54:1871-1881. 10.1007/s11517-016-1478-9
643 Ye H, and Steiger A. 2015. Neuron matters: electric activation of neuronal tissue is dependent on the
644   interaction between the neuron and the electric field. *J Neuroeng Rehabil* 12:65.
645   10.1186/s12984-015-0061-1
646 Yu H, Zheng C, and Wang Y. 2005. A new model and improved cable function for representing the
647   activating peripheral nerves by a transverse electric field during magnetic stimulation.
648   *Proceedings of the 2nd International IEEE EMBS Conference on Neural Engineering*. Arlington,
649   Virginia.
650 Zhao H, Steiger A, Nohner M, and Ye H. 2015. Specific Intensity Direct Current (DC) Electric Field
651   Improves Neural Stem Cell Migration and Enhances Differentiation towards betaIII-Tubulin+
652   Neurons. *PLoS One* 10:e0129625. 10.1371/journal.pone.0129625

653

654 **Figure legends**

655 **Figure 1. Model setup for a myelin-covered axon (A) and a bare axon (B) under transverse**

656 **electric field stimulation.** The cylindrical coordinate system that was used to define the

657 orientation of the electric field and the axon.

658 **Figure 2. Polarization of a myelin-covered axon (A) and a bare axon (B) in a transverse**

659 **electric field.** The *Vm* was calculated by equations 11 and 13, for the myelin-covered axon and

660 the bare axon, respectively. ϕ was calculated by equation 12. All calculations were based on the

661 standard parameters in Table 1. The color maps represented the amount of polarization (in mV).

662 (**C**) Effect of transverse electric field intensity on axonal polarization in myelin-covered and bare

663 axons. (**D**) Log plot of (C).

664

665 **Figure 3. Dependency of *Vm* on the biophysics properties of the axon.** (**A**) Axolemma diameter.

666 (**B**) Axolemma thickness. (**C**) Axolemma conductivity.

667 **Figure 4. Effects of decreased myelin thickness on axonal polarization.** Reduction of myelin

668 thickness from 3.4 μm to 0.1 μm (and linear increase of its conductivity) caused a significant

669 reduction in ϕ, but not *Vm*. For the inset example, axon diameter = 0.6 μm. Myelin thickness = 0.1

670 μm.

671 **Figure 5. Effects of a leaky myelin sheath on axolemma polarization in a transverse electric**

672 **field.** Conductivity of each myelin layer was (**A**) 5×10^{-5} S/m, (**B**) 5×10^{-3} S/m, and (**C**) 5×10^{-1} S/m,

673 respectively. For the inset two examples, axon diameter = 0.6 μm. Myelin diameter = 0.7 μm and

674 4.6 μm, respectively.

675 **List of additional files:**

676 Supplementary file 1 [Mathematic derivations for potential distributions in the five modeled
677 regions in myelin-covered axon (equation 9), and the transmembrane membrane potential *Vm*
678 (equation 11).]

679 Supplementary file 2 [Mathematic derivations for ϕ for the myelin sheath (equation 12).]

680 Supplementary file 3 [Mathematic derivations for *Vm* in the bare axon (equation 13).]

681

Figure 1

Model setup for a myelin-covered axon (A) and a bare axon (B) under transverse electric field stimulation.

The cylindrical coordinate system that was used to define the orientation of the electric field and the axon.
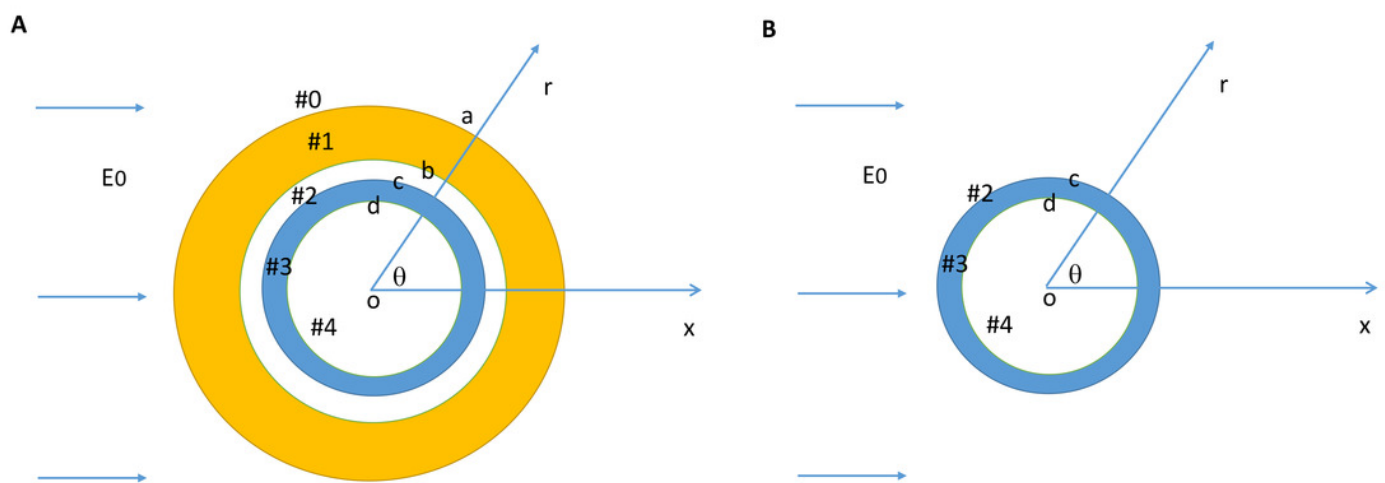
Figure 2

Polarization of a myelin-covered axon (A) and a bare axon (B) in a transverse electric field.

The *Vm* was calculated by equations 11 and 13, for the myelin-covered axon and the bare axon, respectively. *f* was calculated by equation 12. All calculations were based on the standard parameters in Table 1. The color maps represented the amount of polarization (in mV). (**C**) Effect of transverse electric field intensity on axonal polarization in myelin-covered and bare axons. (**D**) Log plot of (C).
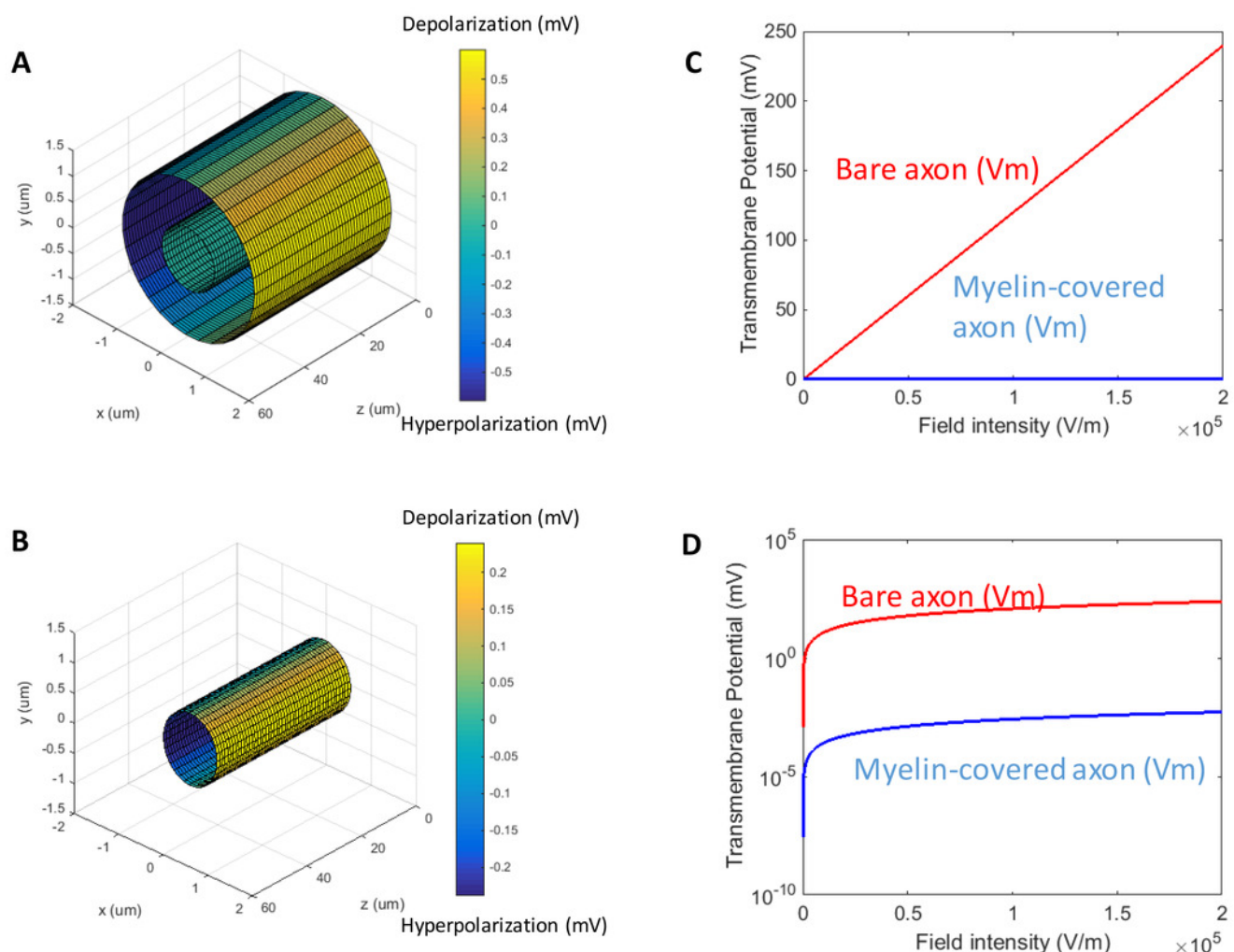
Figure 3

Dependency of *Vm* on the biophysics properties of the axon.

(**A**) Axolemma diameter. (**B**) Axolemma thickness. (**C**) Axolemma conductivity.
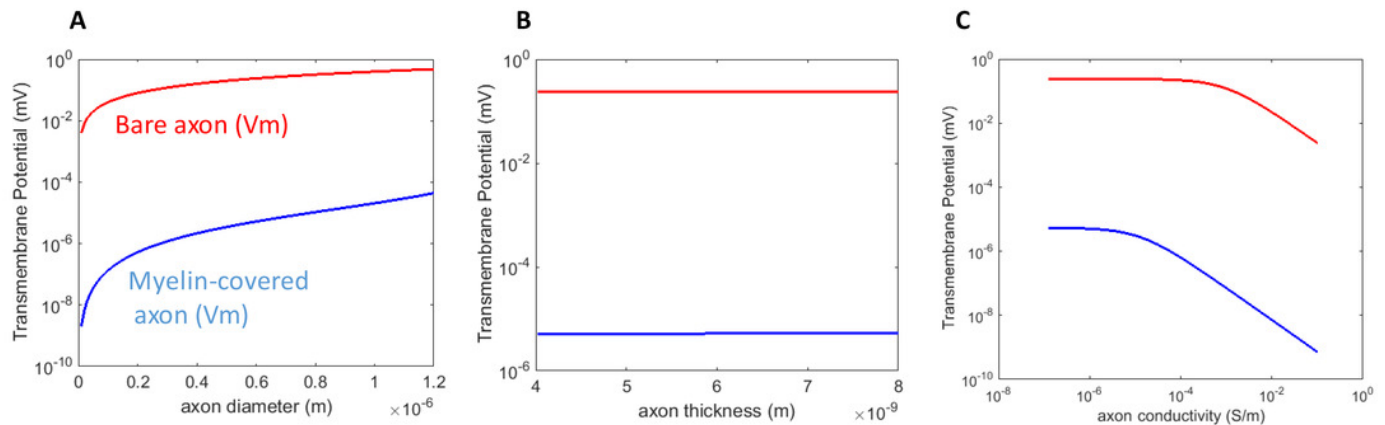
Figure 4

Effects of decreased myelin thickness on axonal polarization.

Reduction of myelin thickness from 3.4 μm to 0.1 μm (and linear increase of its conductivity) caused a significant reduction in f, but not Vm . For the inset example, axon diameter = 0.6 μm. Myelin thickness = 0.1 μm.
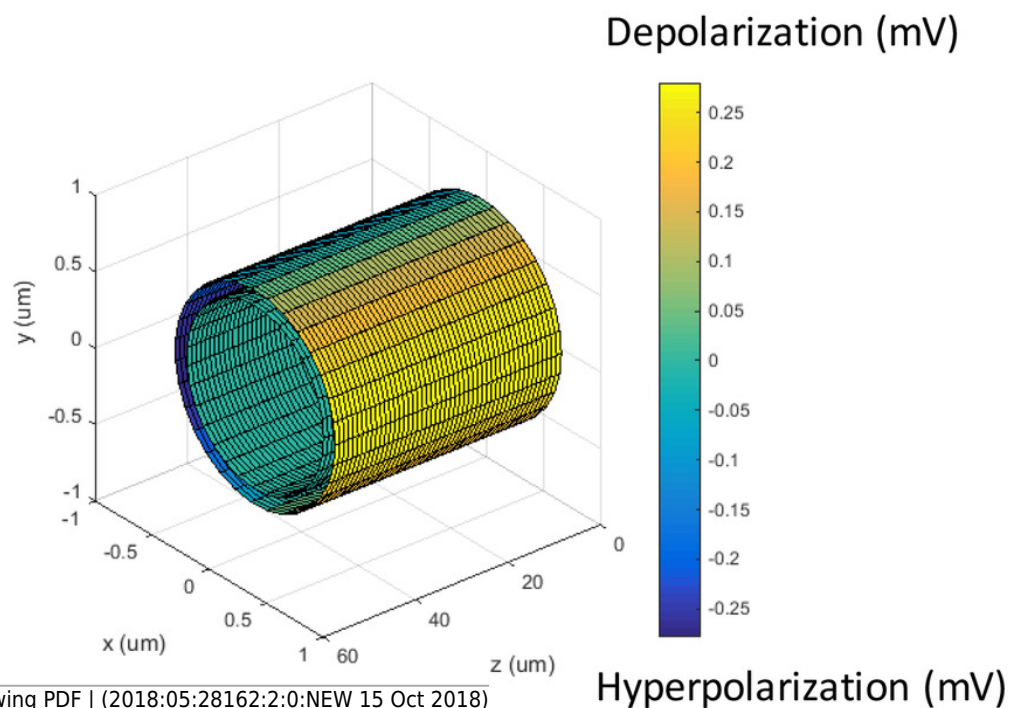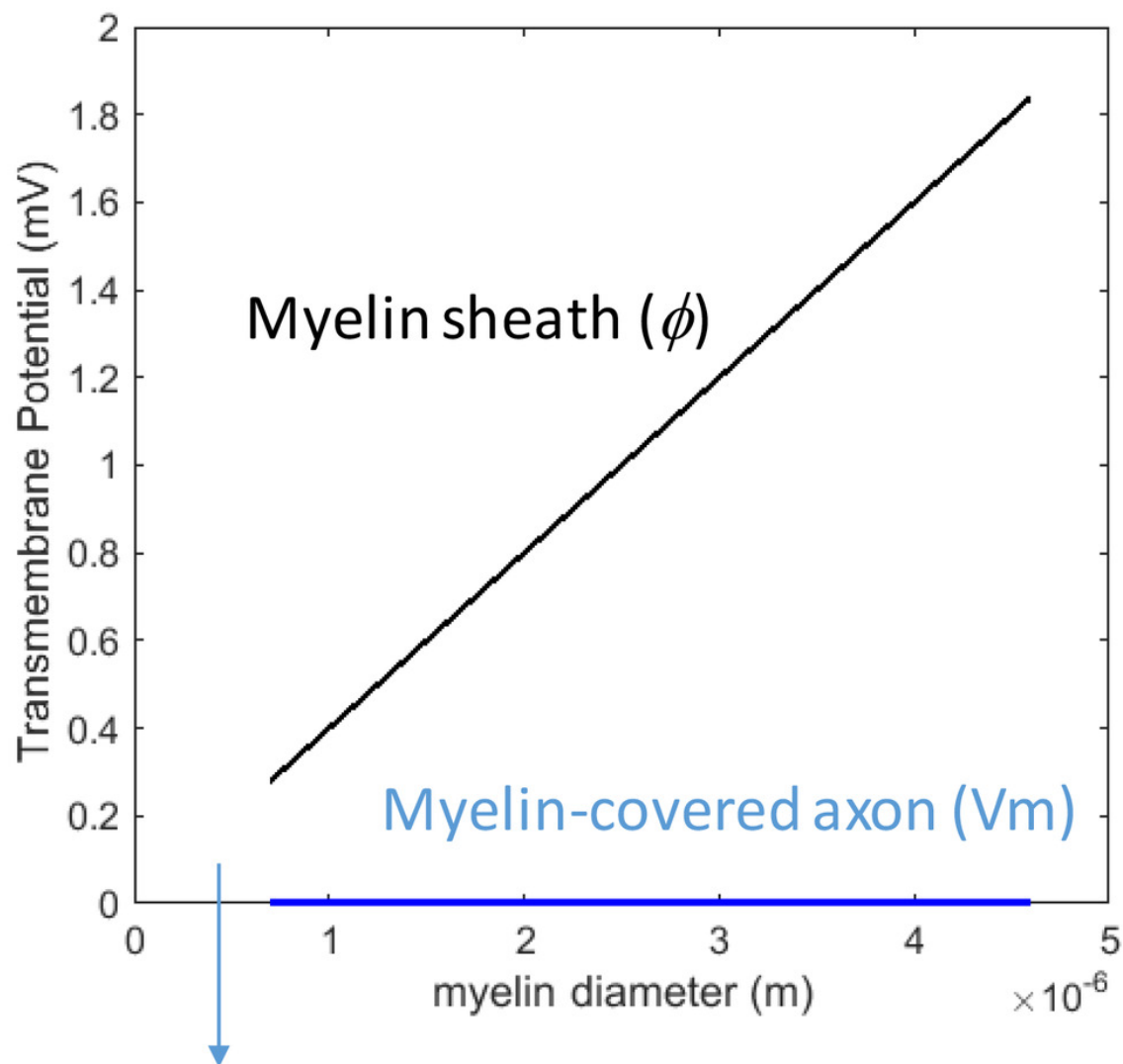
Figure 5

Effects of a leaky myelin sheath on axolemma polarization in a transverse electric field.

Conductivity of each myelin layer was **(A)** 5 ´ 10 $^{-5}$ S/m, **(B)** 5 ´ 10 $^{-3}$ S/m, and **(C)** 5 ´ 10 $^{-1}$ S/m, respectively. For the inset two examples, axon diameter = 0.6 μm. Myelin diameter = 0.7 μm and 4.6 μm, respectively.
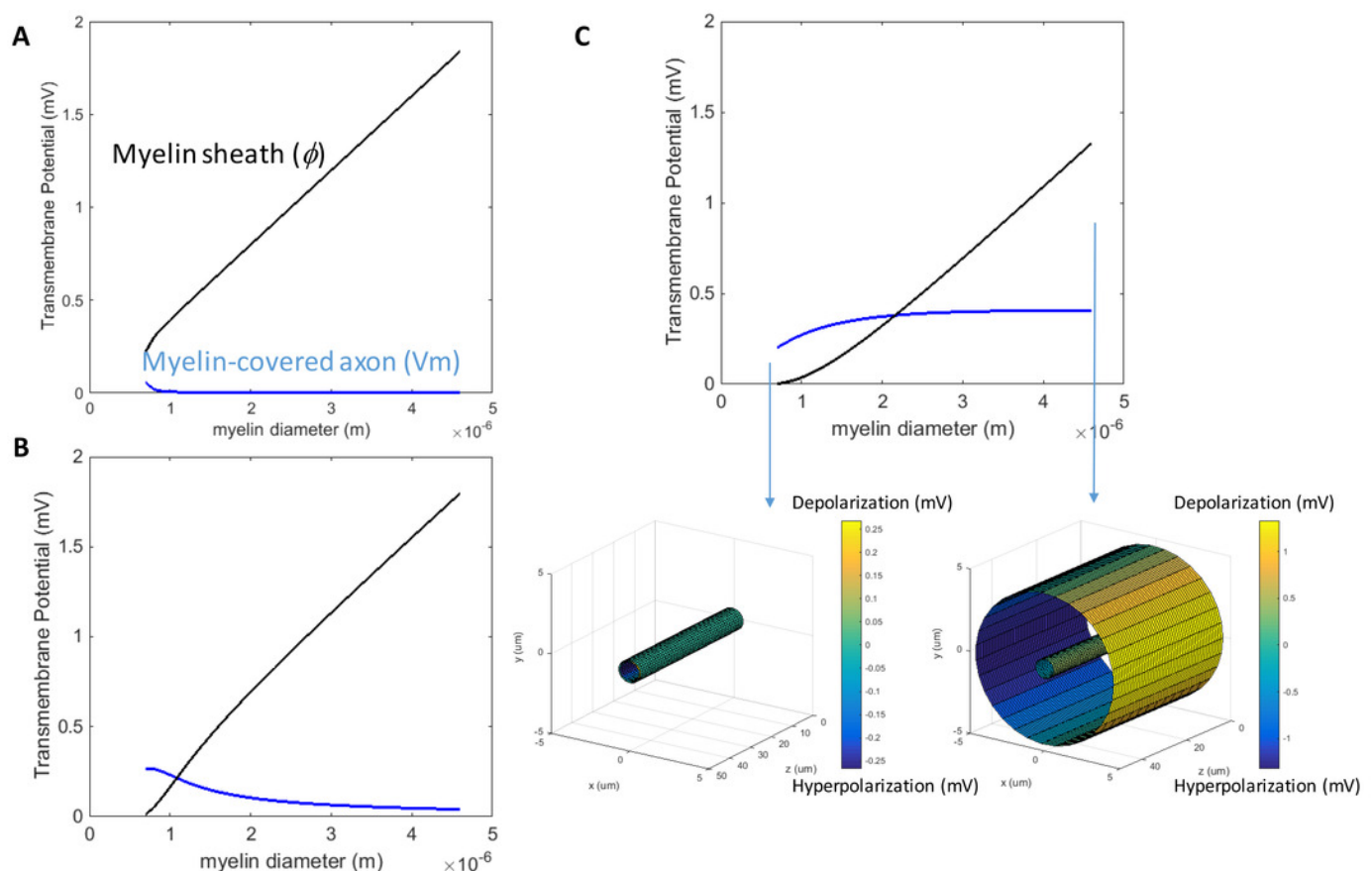
Model parameters.

Parameters	Standard value	Lower limit	Upper limit
Extracellular conductivity (σ_0, S/m) [a,b]	0.2	5×10^{-4}	2.0
Myelin conductivity (σ_1, S/m) [a,b]	$5.0 \times 10^{-7}/n$ [g]	$1.0 \times 10^{-8}/n$	$1.2 \times 10^{-6}/n$
Periaxonal conductivity (σ_2, S/m) [a,b]	0.2	2.0×10^{-2}	1.0
Axonal conductivity (σ_3, S/m) [a,b]	5.0×10^{-7}	1.0×10^{-8}	1.2×10^{-6}
Cytoplasmic conductivity (σ_4, S/m) [a,b]	0.2	2.0×10^{-2}	1.0
Extracellular dielectric permittivity (ε_0, As/Vm) [a,b]	6.4×10^{-10}	3.5×10^{-10}	7.0×10^{-10}
Myelin dielectric permittivity (ε_1, As/Vm) [a,b]	4.4×10^{-11}	1.8×10^{-11}	8.8×10^{-11}
Periaxonal dielectric permittivity (ε_2, As/Vm) [a,b]	6.4×10^{-10}	3.5×10^{-10}	7.0×10^{-10}
Axonal myelin dielectric permittivity (ε_3, As/Vm) [a,b]	4.4×10^{-11}	1.8×10^{-11}	8.8×10^{-11}
Cytoplasmic dielectric permittivity (ε_4, As/Vm) [a,b]	6.4×10^{-10}	3.5×10^{-10}	7.0×10^{-10}
Myelin diameter (a, nm)	1.5	0.7	4.6
b. Axonal membrane thickness (nm)[c]	6	4	8
Axonal radius (c, μm) [d]	0.6	0.1	1.2
Periaxonal space width (μm) [e]	0.004	0.004	0.004

Number of myelin layers (n) [f]	40	0	40
Electric field intensity (V/m)	200	0	200000 [h]

1 [a] (Kotnik et al. 1997).

2 [b] (Kotnik & Miklavcic 2006).

3 [c] (Nagarajan & Durand 1995).

4 [d] (Berthold & Rydmark 1995).

5 [e] (Berthold et al. 1983).

6 [f] (Ruff et al. 2013).

7 [g] (Chomiak & Hu 2009).

8 [h] (Sadik et al. 2011).

10 **Table 1. Model parameters.**